JJEE

Volume 12 | Number 1 | March 2026 | Pages 91-111

Jordan Journal of Electrical Engineering

ISSN (print): 2409-9600, ISSN (online): 2409-9619

Homepage: jjee.ttu.edu.jo

Dual-Elite Social Group Optimization for Enhanced Maximum Power Point Tracking in Partially Shaded Photovoltaic Systems

Houssem Saber Saber[1*], Hammoud Radjeai[2], Abd Elouadoud Bendaouad[3], Lazhar Rahmani[4]

[1, 2, 3, 4] Electric engineering department, LAS Laboratory, Ferhat ABBAS Setif -1 University Setif, Algeria
E-mail: houssem.saber@univ-setif.dz

Received: Jul 10, 2025 *Revised: Dec 08, 2025* *Accepted: Dec 22, 2025* *Available online: Mar 19, 2026*

***Abstract*—** This paper introduces Dual-Elite Social Group Optimization (DE-SGO), A novel version of the standard SGO algorithm for enhanced Maximum Power Point Tracking in photovoltaic systems. Under partial shading conditions, conventional MPPT algorithms often converge to local maxima rather than the Global Maximum Power Point (GMPP) due to multi-peak power-voltage characteristics, resulting in significant energy harvest losses. The proposed DE-SGO addresses this limitation by implementing structured knowledge transfer from both the best and second-best solutions simultaneously, creating a hierarchical learning structure that enhances exploration and exploitation capabilities. The novel proposed algorithm has been implemented in MATLAB Simulink using SPM0409 photovoltaic specifications and evaluated against standard SGO, Cuckoo Search Optimization CSO, Particle Swarm Optimization PSO, and Teaching-Learning-Based Optimization TLBO across three scenarios: rapid irradiance fluctuations, moderate partial shading with a centrally located GMPP, and severe partial shading with a rightward-shifted GMPP. The simulation results demonstrate that DE-SGO consistently outperforms competing algorithms in both tracking efficiency (achieving up to 99.71% under severe partial shading) and convergence speed (0.18-0.23 seconds compared to 0.32-0.72 seconds for other methods). The algorithm exhibits superior performances in terms of dynamic response characteristics, with low oscillations around the MPPT, and more stable duty cycle control. The obtained results without additional hardware or complex implementation. Offering a robust solution for maximizing energy harvest in applications where non-uniform irradiance is common, particularly in systems experiencing frequent environmental variations.

***Keywords*—** Solar energy; Photovoltaic systems; DE-SGO; SGO; MPPT; Optimization algorithms; Partial shading.

1. INTRODUCTION

Photovoltaic (PV) systems have emerged as a prominent renewable energy source due to their scalability, decreasing costs, and minimal environmental impact [1]. However, maximizing power extraction from PV systems remains challenging, particularly under non-uniform irradiance conditions [2]. Partial shading conditions (PSCs) create multiple power peaks on the power-voltage (P-V) curve, causing conventional Maximum Power Point Tracking (MPPT) algorithms to become trapped in local maxima rather than identifying the Global Maximum Power Point (GMPP) [3].

Traditional MPPT algorithms, including Perturb and Observe (P&O), Incremental Conductance (INC), and Hill Climbing (HC), have been widely employed in PV systems due to their simplicity and ease of implementation[4]. These conventional techniques demonstrate satisfactory performance under uniform irradiance conditions but exhibit significant limitations under partial shading conditions [5]. The presence of multiple local maxima in the P-V characteristic curve causes these gradient-based algorithms to converge to suboptimal

* Corresponding author
DOI: https://doi.org/10.5455/jjee.204-1752171111

power points, resulting in substantial power losses. Furthermore, they suffer from steady-state oscillations around the maximum power point and are susceptible to environmental noise, necessitating the development of more sophisticated tracking approaches [6].

In recent years, metaheuristic optimization algorithms have gained significant attention for addressing the MPPT challenge under PSCs due to their ability to navigate complex, non-linear search spaces [7]. Various approaches have been proposed, including Particle Swarm Optimization (PSO), Social Group Optimization (SGO), Cuckoo Search Optimization (CSO), and Teaching-Learning-Based Optimization (TLBO) [8-10] . Despite their effectiveness, these algorithms often face limitations in balancing exploration and exploitation, resulting in either reduced tracking accuracy or extended convergence times [11].

The Social Group Optimization (SGO) algorithm inspired by knowledge transfer mechanisms in human social groups, has demonstrated promising results in MPPT applications [12]. SGO operates through two primary phases: the Improving phase, where individuals enhance their knowledge based on the best performer in the group, and the Acquiring phase, where individuals learn through random interactions with other members [13]. While effective, the standard SGO's reliance on random interactions in the Acquiring phase can introduce inefficiencies in the search process, potentially delaying convergence to the GMPP [14].

This paper introduces a novel modification to the SGO algorithm, termed Dual-Elite SGO (DE-SGO), which enhances the Acquiring phase by implementing a structured knowledge transfer mechanism. Unlike the standard SGO, where candidates interact with randomly selected members, the proposed DE-SGO employs a dual-source knowledge acquisition approach where candidates systematically learn from both the best and second-best performers in the population. This hierarchical learning structure creates a more efficient knowledge propagation pathway that accelerates convergence while maintaining the algorithm's ability to escape local maxima [15].

The main contributions of this work encompass the development of a structured dual-source knowledge transfer mechanism that enhances the SGO algorithm's performance in MPPT applications without increasing computational complexity, comprehensive evaluation of the proposed DE-SGO against established metaheuristic techniques across multiple challenging scenarios that reflect real-world operational conditions [16], detailed analysis of performance improvements in both tracking efficiency and convergence speed, particularly under complex partial shading conditions with multiple local maxima, and implementation validation using industry-standard PV module specifications to demonstrate practical applicability [17].

The proposed DE-SGO algorithm demonstrates substantial performance improvements over existing metaheuristic approaches. Evaluation results reveal that DE-SGO achieves up to 99.93% tracking efficiency under severe partial shading conditions while reducing convergence time compared to standard SGO and by 99.78% compared to PSO and TLBO implementations. The algorithm's enhanced dual-source knowledge transfer mechanism enables superior exploration-exploitation balance, facilitating more effective escape from local maxima while maintaining rapid convergence toward the global maximum power point. These findings indicate significant practical value for renewable energy applications, offering a computationally efficient solution that maximizes energy harvest without requiring additional hardware components or complex implementation strategies.

The remainder of this paper is organized as follows: Section 2 details the standard SGO algorithm and introduces the proposed DE-SGO modification. Section 3 presents the implementation of Dual-Elite Social Group Optimization for Maximum Power Point Tracking. Section 4 describes the simulation framework and experimental setup. Finally, Section 5 presents and discusses the comparative results across three distinct test scenarios.

2. DUAL-ELITE SOCIAL GROUP OPTIMIZATION ALGORITHM (DE-SGO): DESCRIPTION AND PHASES.

2.1. Introduction

The Social Group Optimization (SGO) algorithm is a population-based metaheuristic inspired by the knowledge transfer mechanisms observed in human social groups. SGO emerged from leveraging the competencies of individuals in groups, where some members possess superior problem-solving capabilities and yield optimized solutions [12]. When these knowledgeable individuals are part of a social group, other members acquire cognizance from them and emulate successful problem-solving approaches [18].

This work proposes a significant modification to the standard SGO framework, specifically enhancing the Acquiring phase through a structured knowledge transfer pattern [19]. Unlike the original SGO algorithm where interactions between candidates occur randomly, Dual-Elite Social Group Optimization (DE-SGO) implements a deterministic knowledge transfer mechanism that involves both the best and second-best candidates. This modification aims to improve convergence efficiency and solution quality by creating a more structured flow of knowledge throughout the population [20].

2.2. Population Structure

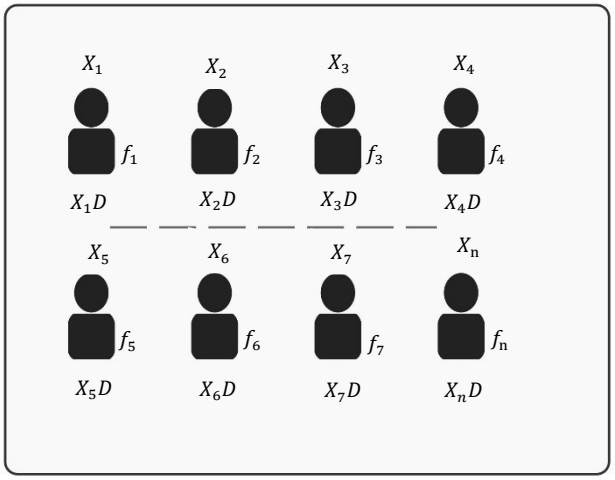

Fig. 1. Population structure of N candidates in the SGO algorithm.

As illustrated in Fig. 1, the algorithm maintains a population of N individuals (X_1, X_2, ..., X_n,), each representing a candidate solution to the optimization problem under consideration [12]. Each candidate X_K, possesses:

- A specific position in the D-dimensional search space, denoted as $X_K D$, representing the solution parameters.
- An associated fitness value f_k that quantifies the quality of the solution.

The number of members in the group is termed as N, each individual is termed as X_K, where k represents the specific candidate number in that group. $X_K D$ refers to the dimension of the candidate, which is a reference to the qualities of the individual, and f_K (k = 1, 2, ..., N) is their associated fitness value [18].

2.3. Algorithm Phases

The SGO algorithm consists of two primary phases: the Improving phase and the Acquiring phase. In the first phase, the knowledge of each individual candidate is improved through impact acquired from the best person within the group. In the second phase, each candidate improves its knowledge through interactions with other members of the group and the overall best person [21].

Dual-Elite Social Group Optimization (DE-SGO) algorithm retains this fundamental two-phase structure while introducing a strategic enhancement to the knowledge acquisition mechanism in the second phase.

2.4. Improving Phase

In this phase, each social group's best candidate is called the global best (Gbest) and disseminates knowledge to other team members, as illustrated in Fig. 2. The best candidate (X_2 in red with a yellow star) with the highest fitness value is identified. The team members that participate in this learning enhance their knowledge [22].

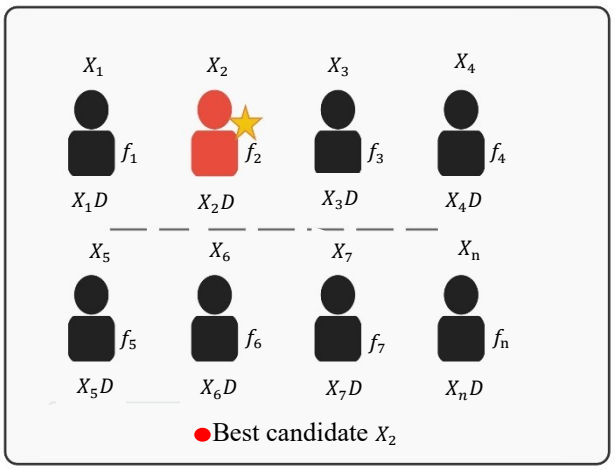

Fig. 2. Best candidate identification in the DE-SGO algorithm.

The fitness function for maximization is $Gbest = \max\{f(X_k), \mathrm{k} = 1, 2, \ldots, \mathrm{N}\}$. During this phase, for every iteration, the knowledge between the candidates is shared and updated, which can be represented by the following equation [23]:

$$Xnew_{kj} = C \times Xold_{kj} + r \times \left(Gbest(j) - Xold_{kj}\right) \quad (1)$$

where:

- $Xnew_{kj}$ represents the updated position of the k^{th} candidate in the j^{th} dimension.
- C is a self-introspection parameter.
- r is a random number within [0,1].
- $Gbest(j)$ is the j^{th} dimension of the global best solution.

This phase follows the standard SGO approach, where each individual attempts self-improvement through knowledge gained from the best-performing candidate. The candidate accepts the new position only if it yields an improved fitness value.

2.5. Acquiring Phase in Standard SGO

In the standard SGO algorithm, each member of the group obtains knowledge from the highly knowledgeable person $gbest$ and also interacts with other members selected randomly.

The candidates acquire new knowledge from each other as well as from the most knowledgeable person. If another individual develops more knowledge than the current $gbest$, then it replaces the best candidate [19].

The process involves randomly selecting one person X_r, where j ≠ r, and applying the following update rules [24]:

If $f(X_k) > f(X_r)$:

$$Xnew_{k,j} = Xold_{k,j} + r1 \times \left(X_{k,j} - X_{r,j}\right) + r2 \times \left(Gbest_j - Xold_{k,j}\right) \quad (2)$$

$f(X_k) < f(X_r)$:

$$Xnew_{k,j} = Xold_{k,j} - r1 \times \left(X_{k,j} - X_{r,j}\right) + r2 \times \left(Gbest_j - Xold_{k,j}\right) \quad (3)$$

Accept $Xnew$ if it gives a better fitness function value, where $r1$ and $r2$ are two independent random sequences that influence the algorithm's stochastic nature.

2.6. Modified Acquiring Phase (DE-SGO)

The significant contribution of this work lies in the modification of the Acquiring phase. As illustrated in Fig. 3, the DE-SGO implements a more structured knowledge transfer mechanism where the best candidate (X_2, highlighted in red) directly transfers knowledge to other candidates (such as X_7, highlighted in blue) through a systematic interaction pattern (represented by the purple dashed arrow).

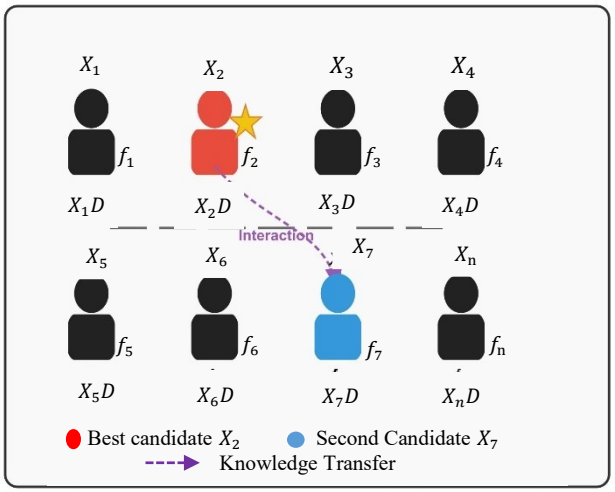

Fig. 3. Best Knowledge transfer from best candidate in Dual-Elite Social Group Optimization algorithm.

However, the full modification goes beyond this single interaction. In the DE-SGO, we introduce an additional enhancement to the knowledge transfer mechanism.

As shown in Fig. 4, each candidate in the DE-SGO acquires knowledge not only from the best candidate (X_2, in red) but also systematically interacts with the second-best candidate (X_3, in green). The purple dashed arrow shows knowledge transfer from the best candidate to the third candidate (X_7, in blue), while the orange dashed arrow represents knowledge transfer from the second-best candidate to the same target.

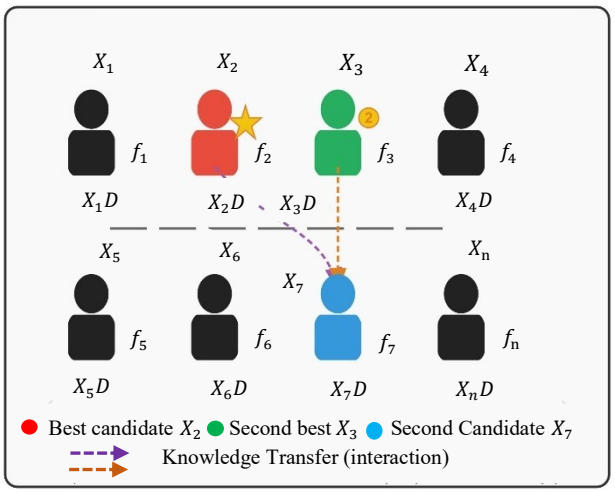

Fig. 4. Dual knowledge transfer in Dual-Elite Social Group Optimization algorithm.

This dual-source knowledge acquisition replaces the random interactions in the standard SGO with a deterministic approach. The mathematical formulation of this modified approach can be expressed as:

$$Xnew_{k,j} = Xold_{k,j} + r1 \times \left(Xsecbest_j - X_{r,j}\right) + r2 \times \left(Gbest_j - Xold_{k,j}\right) \quad (4)$$

where:

- $Xsecbest_j$ represents the j^{th} dimension of the second-best candidate.
- $r1$ and $r1$ are random numbers controlling the influence of each knowledge source.

The DE-SGO maintains the dynamic leadership principle of SGO, where if any candidate develops a superior solution than the current best, it assumes the position of the global best (Gbest).

3. TECHNICAL DIFFERENTIATION FROM RELATED OPTIMIZATION METHODS

Recent MPPT research has explored advanced PSO variants and hybrid optimization strategies. Othman et al. (2024) developed PSO-based adaptive sliding mode control where particle velocity dynamics incorporate both individual best and global best guidance, requiring careful tuning of inertia weight, cognitive coefficient, and social coefficient parameters throughout the convergence process [25]. Regaya et al. (2024) proposed multiswarm PSO with adaptive factor selection strategy, dividing the population into separate subswarms each with independent search behaviors and requiring dynamic leader selection among subgroups to coordinate exploration-exploitation balance [26]. Zaghba et al. (2025) presented hybrid fuzzy-PI MPPT where PSO optimizes controller parameters through iterative fitness evaluations, necessitating coordination between fuzzy rule-based systems and PSO population management [27]. Chtita et al. (2022) combined grey wolf encircling behavior using hierarchical alpha-beta-delta wolf positions with PSO velocity dynamics, requiring parallel operation of two distinct algorithmic frameworks with separate parameter sets [28].

DE-SGO employs fundamentally different update mechanics. The Improving phase implements direct position updates based on current position, self-introspection parameter, and distance to best solution, completely eliminating velocity vectors and associated inertia weight tuning. The modified Acquiring phase introduces deterministic dual-source learning where each candidate receives simultaneous guidance from both best and second-best solutions through additive position adjustments with independent random factors. This flat dual-elite structure contrasts with multiswarm architectures requiring hierarchical subgroup divisions

and dynamic leader reassignment. The absence of velocity dynamics removes traditional exploration-exploitation balance dependency on inertia weight scheduling found in PSO variants. Unlike hybrid approaches coordinating multiple algorithmic frameworks, DE-SGO achieves dual-source learning within a single unified update mechanism requiring only three parameters. The deterministic dual-source guidance eliminates stochastic leader selection complexity while providing structured knowledge transfer without external archive maintenance or mutation operations.

4. IMPLEMENTATION OF DUAL-ELITE SOCIAL GROUP OPTIMIZATION FOR MAXIMUM POWER POINT TRACKING

This section presents the implementation framework of the Dual-Elite Social Group Optimization (DE-SGO) algorithm for tracking the Global Maximum Power Point (GMPP) in photovoltaic systems. The DE-SGO-MPPT configuration comprises a photovoltaic array connected to a load via a boost converter, with the control signal derived from the proposed algorithm operating within a dedicated microcontroller [13]. The controller processes real-time voltage and current measurements to calculate the optimal duty cycle for GMPP identification.

4.1. Initialization Phase

The algorithm begins with population initialization:

Step 1: Generate a population of N candidate duty cycles $\{D_1, D_2, \ldots, D_n\}$ distributed within the operational range $[D_{min}, D_{max}]$. Each duty cycle represents a potential solution to the MPPT problem.

Pseudocode - Initialization Phase:

for i = 1 to N do
$D_i = D_{min}$ + rand() × (D_{max} - D_{min})
end for

4.2. Improving Phase

During this phase, candidates improve their fitness through interaction with the best-performing solution:

Step 2: Measure the power output $P(D_i)$ for each duty cycle candidate when applied to the converter. Identify the duty cycle yielding maximum power as the global best solution ($Gbest$).

Each controle update requires N power measurements (one per duty cycle candidate). For N=4 agents needs 4 voltage and 4 current measurements.

Step 3: Update each candidate solution according to the following mathematical formulation:

$$Dnew_i = C \times Dold_i + r \times (Gbest - Dold_i) \quad (5)$$

where:

- $Dnew_i$ represents the updated duty cycle
- C denotes the self-introspection parameter [0,1]
- r is a stochastic coefficient [0,1]
- The term ($Gbest - Dold_i$) represents the knowledge gradient between the best candidate

and the current solution

The updated solution replaces its predecessor conditionally upon demonstrating superior performance. The coefficients C and r are dynamically adjusted throughout the optimization process to maintain an appropriate balance between exploration and exploitation [29].

Pseudocode - Improving Phase:

// Measure power for all candidates (N measurements)
for i = 1 to N do
    Apply duty cycle D_i to converter
    Measure V_{pv}(i) and I_{pv}(i) // 2 measurements
    Calculate P(i) = V_{pv}(i) × I_{pv}(i)
end for
// Identify best candidate
$Gbest = D_i$ with maximum P(i)
// Update each candidate
for i = 1 to N do
    r = rand (0,1)
    $Dnew_i = C \times Dold_i + r \times (Gbest - Dold_i)$ /Eq. (5)
    Ensure $Dnew_i \in [D_{min},\ D_{max}]$
    if P($Dnew_i$) > P(D_i) then
        $D_i = Dnew_i$
    end if
end for

4.3. Modified Acquiring Phase

This phase incorporates the key modification to the standard SGO algorithm:

Step 4: Each candidate solution enhances its position through structured interactions with both the best and second-best solutions, rather than random candidate selection. This process is mathematically expressed as:

$$Dnew_i = Dold_i - r1 \times (Dsecbest - Dold_i) + r2 \times (Gbest - Dold_i) \quad (6)$$

where:

- $Dsecbest$ represents the duty cycle of the second-best candidate.
- $r1$ and $r2$ are independent stochastic parameters [0,1].
- This formulation facilitates hierarchical knowledge transfer from both premier solutions.

Step 5: Update the new $Gbest$ and $Dsecbest$ based on the latest power measurements.

The optimal duty cycle detection process involves initialization of multiple duty cycles (D_1, D_2, D_3, D_4, ...). The value of each duty cycle is computed using Eq. (5) during the improving phase. The respective power measurements for these duty cycles are recorded, with the duty cycle producing maximum power designated as the global best $Gbest$, and the second-highest power producer as $Dsecbest$.

The knowledge sharing between $Gbest$, $Dsecbest$, and other candidates occurs through Eq. (6). Each updated duty cycle (candidate) is applied to the power converter, which delivers the corresponding power after each iteration. This search process continues for the

predetermined number of iterations. If the current position of a candidate becomes the best, the peak power value and $Gbest$ are updated accordingly, with consequent updates to $Dsecbest$ as well.

The DE-SGO-MPPT procedure continues until convergence criteria are met, typically when all candidates converge to the vicinity of the GMPP. This structured knowledge transfer mechanism enhances the algorithm's ability to escape local maxima during partial shading conditions by leveraging knowledge from both the best and second-best performers, rather than relying on random interactions that might introduce inefficiencies in the search process.

The convergence of duty cycles with respect to instantaneous voltage and current measurements is particularly significant during partial shading of PV panels, where multiple power peaks may exist. The modified algorithm demonstrates enhanced capability in distinguishing between local and global maxima through its hierarchical knowledge transfer structure.

Pseudocode - Modified Acquiring Phase

```
// Update elite solutions
Gbest = D_i with maximum P(i)
Dsecbest = D_i with second maximum P(i)
// Dual-elite knowledge transfer
for i = 1 to N do
    r1 = rand(0,1)
    r2 = rand(0,1)
    Dnew_i = Dold_i − r1 × (Dsecbest − Dold_i) + r2 × (Gbest − Dold_i)        // Eq. (6)
    Ensure Dnew_i ∈ [D_min, D_max]
    if P(Dnew_i) > P(D_i) then
        D_i = Dnew_i
    end if
end for
// Check convergence
if |P(Gbest, new new) - P(Gbest, old)| < ε then
    converged = true
end if
```

4.4. Computational Complexity and Real-Time Feasibility

The computational efficiency of DE-SGO is critical for real-time MPPT implementation. The algorithm exhibits (N × M) complexity, where N represents population size and M denotes iterations to convergence.

For N=4 agents, each iteration requires approximately 4 power calculations (P = V × I) involving 4 multiplications, elite identification requiring 4 comparisons, an improving phase performing 12 multiplications and 8 additions, and an acquiring phase executing 16 multiplications and 12 additions, totaling approximately 32 multiplications, 20 additions, and 4 comparisons per iteration.

As demonstrated in Fig. 5, DE-SGO converges in 4.7-5.2 iterations on average, resulting in approximately 244-270 total operations per MPPT cycle. Estimated execution time on a typical MCU shows that a single iteration requires approximately 20-30 µs (including ADC sampling), while a complete MPPT cycle executes in approximately 100-150 µs. Given the typical MPPT control period requirement of 10-100 ms.

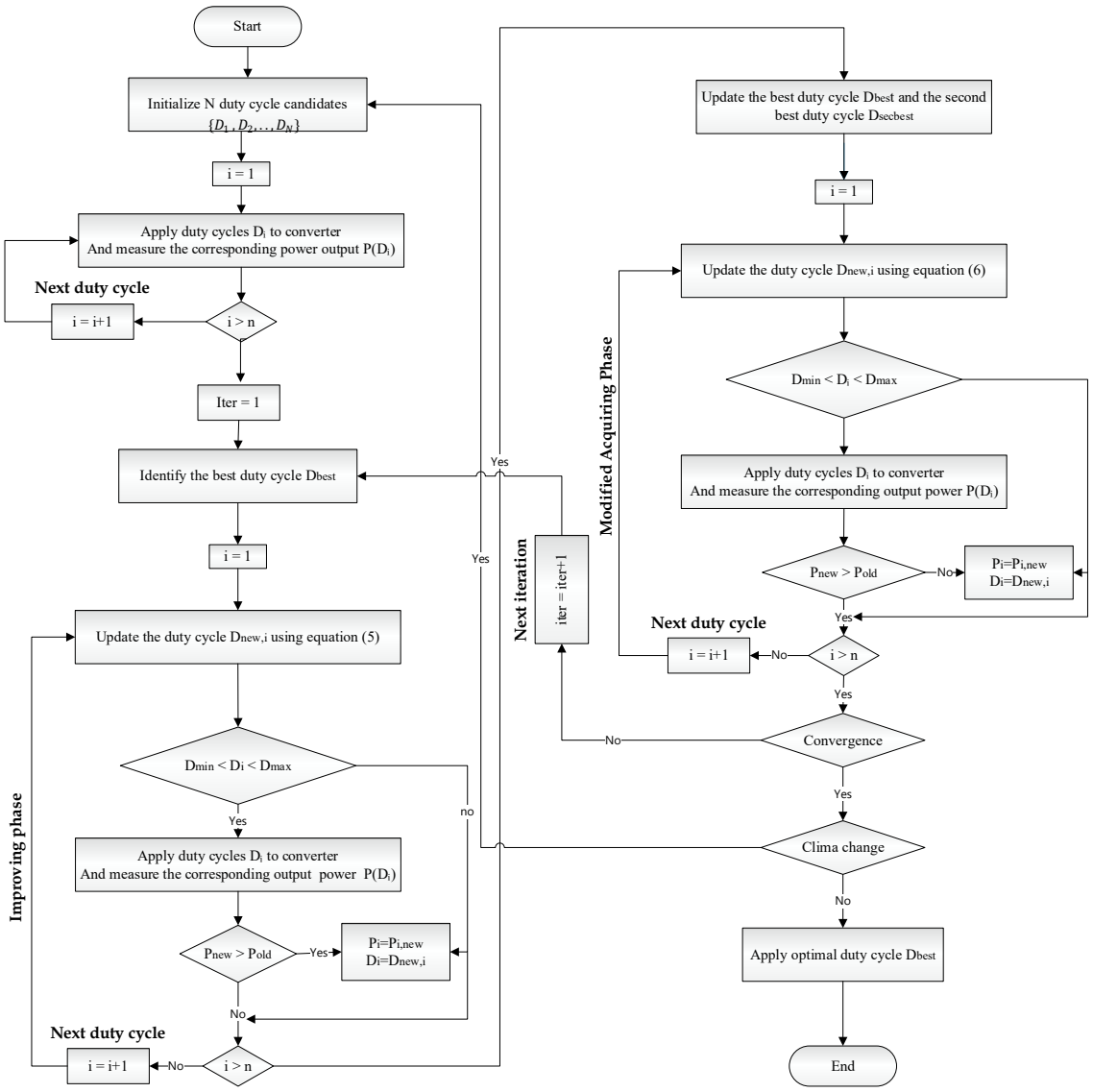

Fig. 5. Operational flow chart of DE-SGO-MPPT process.

5. SIMULATION RESULTS AND DISCUSSION

5.1. Algorithm Performance Evaluation and Comparative Analysis

This section presents a detailed analysis of the Dual-Elite Social Group Optimization (DE-SGO) algorithm's performance across three distinct scenarios implemented under MATLAB Simulink, see Fig. 6. The comparative evaluation examines DE-SGO against established metaheuristic techniques including Social Group Optimization (SGO), Cuckoo Search Optimization (CSO), Particle Swarm Optimization (PSO), and Teaching-Learning-Based Optimization (TLBO). These reference algorithms serve as benchmarks for quantifying DE-SGO's effectiveness in identifying Global Maximum Power Points (GMPP) under varying operational conditions. The simulation scenarios progressively increase in complexity from rapid irradiance variations to moderate and severe partial shading conditions, providing a comprehensive assessment of each algorithm's tracking efficiency, convergence speed, and control stability.

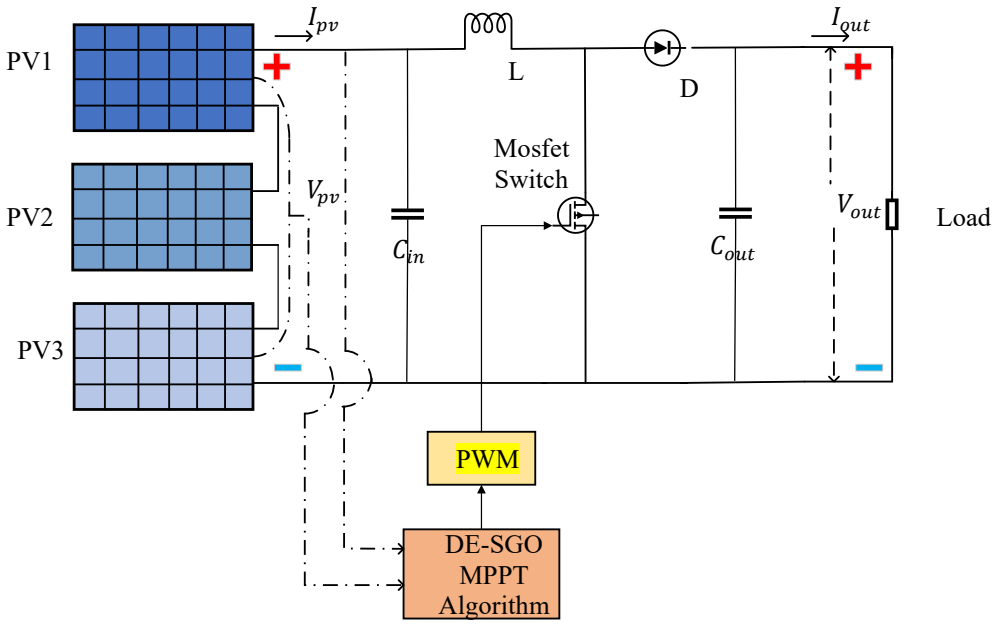

Fig. 6. Simulink model of PV system.

The experimental validation employs the SPM0409 photovoltaic module specifications from Kyocera Corporation to ensure fidelity with real-world implementation. The simulation parameters incorporate the manufacturer's datasheet values under Standard Test Conditions (STC), as detailed in Table 1, thereby establishing a realistic foundation for performance evaluation and comparative analysis.

Table 1. PV module specifications.

Parameters	Value
Maximum Power (P_{max})	90 W
Maximum Power Voltage (V_{mp})	19.64 V
Maximum Power Current (I_{mp})	4.59 A
Open Circuit Voltage (V_{oc})	24.6 A
Short Circuit Current (I_{sc})	5.03 A
Series resistance of PV model (R_s)	5.96 Ω
Parallel resistance of PV model (R_{sh})	62.4 Ω
Number of Cells per Module	36

For the DC-DC power conversion stage, a boost converter topology was implemented due to its ability to step up the PV array voltage to match load requirements while providing continuous input current with low ripple, making it ideal for MPPT applications. The converter was configured with precisely calibrated component values:

The inductor value L of 10 mH ensures continuous conduction mode operation with current ripple ΔIL less than 40% of rated current.

The input capacitor C_{in} of 6 µF minimizes input voltage ripple from the PV array, while the output capacitor C_{out} of 60 µF maintains output voltage ripple below 2% of nominal value, load resistance R of 50 Ω. The switching frequency of 15 kHz provides an optimal balance between converter efficiency and component size.

The boost converter's duty cycle serves as the control variable for the MPPT algorithms, allowing direct manipulation of the PV operating point to track the maximum power point.

Table 2. Boost converter parameters.

Parameters	Value
Inductor L	10 mH
Input capacitor C_{in}	6 µF
Output capacitor C_{out}	60 µF
Switching Frequency	15 kHz
Load Resistance R	50 Ω

Table 3 delineates the optimization parameters configured for the DE-SGO, SGO, CSO, PSO, and TLBO algorithms. To ensure equitable comparison, a uniform initial population size of four agents was established across all metaheuristic MPPT implementations.

Table 3. Tuning parameters for MPPT algorithms under comparison.

MPPT Method	Tuning Parameters
DE-SGO	C_{min}= 0.1, C_{max} = 0.9
SGO	C_{min}= 0.1, C_{max} = 0.9
CSO	Beta=3/2, Kcoeff= 0.8, Sigmav=1
PSO	C_1 = 1.025, C_2 = 1.025, W = 0.4
TLBO	$T_f = 1$

To rigorously assess algorithm performance, three distinct testing scenarios were designed, as detailed in Table 4. Each scenario imposes specific irradiance patterns across the three-panel PV array. Case 1 features rapidly changing uniform irradiance to evaluate dynamic response characteristics. Cases 2 and 3 introduce partial shading conditions with different complexity levels—Case 2 positions the Global Maximum Power Point (GMPP) in the middle of the P-V curve, while Case 3 places the GMPP on the right side. These configurations create progressively challenging optimization problems that effectively test each algorithm's ability to distinguish between local and global maxima under realistic operating conditions.

Table 4. PV panels configuration and insolation levels.

Case Study	Tuning Parameters		
	PV1	PV2	PV3
Case 1, Insolation level	1000,700,400	1000,700,400	1000,700,400
Case 2, Insolation level	1000	700	300
Case 3, Insolation level	900	600	700

The theoretical Global Maximum Power Point (GMPP) values for each test scenario were determined using MATLAB/Simulink PV modeling with parameters from the SPM0409 module datasheet Table 1.

The PV array, consisting of three series-connected modules, was modeled using the single-diode equivalent circuit. For each irradiance pattern, the complete power-voltage (P-V) characteristic was generated by sweeping the array voltage from 0 to open-circuit voltage. The theoretical GMPP was identified as the maximum point on the resulting P-V curve.

Under uniform irradiance (Case 1), the GMPP scales linearly with irradiance level. For partial shading conditions (Cases 2 and 3), the P-V curve exhibits multiple local maxima due to bypass diode activation, and the GMPP was identified as the highest peak among these local maxima. These theoretical values serve as the benchmark for evaluating MPPT tracking efficiency, defined as the ratio of actual extracted power to theoretical GMPP.

5.1.1. Case 1 Analysis: Comparative Performance Under Rapidly Fluctuating Irradiance Conditions

The first case examines the performance of five metaheuristic optimization algorithms (DE-SGO, SGO, CSO, PSO, and TLBO) under rapidly changing solar irradiance conditions. The experimental setup features a three-tier irradiance profile, beginning at a high intensity of 1000 W/m² for 2 seconds, decreasing to 700 W/m² for 2 seconds, and finally dropping to 400 W/m². Figure 7(a) illustrates the power output response of each MPPT technique across the test duration. The theoretical Global Maximum Power Points (GMPPs) corresponding to the three irradiance levels were measured at 270, 186.7, and 100.84 W respectively. The experimental results demonstrate that DE-SGO achieved the highest power extraction at 269.8 W, followed closely by CSO (269.48 W), SGO (269.4 W), TLBO (269.39 W), and PSO (269.38 W). These values translate to harvesting efficiencies of 99.92%, 99.77%, 99.77%, 99.76%, and 99.74% respectively.

Tracking speed emerges as another critical performance metric in this scenario. The DE-SGO algorithm demonstrated superior convergence with a settling time of 0.20 s, outpacing SGO (0.28 s), CSO (0.31 s), TLBO (0.72 s), and PSO (0.76 s). This indicates that DE-SGO not only extracts more power but does so with enhanced temporal efficiency.

The voltage, current, and duty cycle dynamics displayed in Figs. 7(b-d) provide additional insights into the transient behavior of each control mechanism. During transition periods between irradiance levels, all algorithms exhibit oscillatory behavior as they search for new operating points. However, DE-SGO consistently demonstrates more rapid stabilization and reduced oscillation amplitude compared to its counterparts.

Of particular note is the behavior observed in the duty cycle graph, where DE-SGO maintains more consistent operation with fewer extreme excursions during transitional phases. This characteristic contributes to its superior overall performance by reducing energy losses associated with hunting behavior and overshooting target values.

The comparative analysis reveals that while all tested algorithms successfully track maximum power points under rapidly changing conditions, DE-SGO demonstrates marginal but consistent advantages in both static efficiency and dynamic response characteristics.

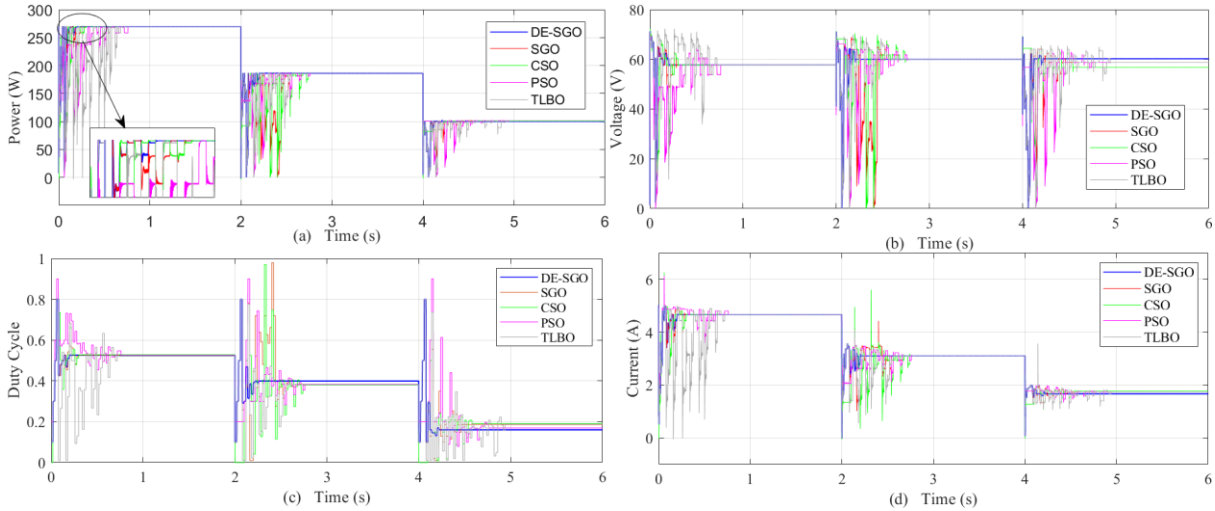

Fig. 7. Comparison of a) power; b) voltage; c) current; and d) duty cycle of DE-SGO, SGO, SCO, PSO, and TLBO under rapidly fluctuating irradiance conditions.

5.1.2. Case 2 Analysis: Algorithm Performance Under Partial Shading

The Second case evaluates the performance of five optimization algorithms (DE-SGO,

SGO, CSO, PSO, and TLBO) under non-uniform irradiation that simulates partial shading conditions. The test applies to a complex irradiation profile with multiple local maximum power points, creating a challenging scenario where algorithms must distinguish between local and global maxima.

As shown in Fig. 8, all five algorithms demonstrate oscillatory behavior during their search for the global maximum power point (GMPP), which is situated in the middle of the P-V curve. The theoretical maximum power under these conditions was calculated to be 132.85W Visual analysis of the power response curves in Fig. 8(a) indicates that DE-SGO achieves the most efficient tracking performance, followed closely by SGO. The measured power extraction values are 132.82W for DE-SGO, 132.81W for CSO, 132.77W for PSO, 132.74W for SGO, and 132.71W for TLBO, corresponding to tracking efficiencies of 99.97%, 99.96%, 99.93%, 99.91%, and 99.89% respectively.

The settling time metrics reveal significant differences in convergence speed among the algorithms. DE-SGO demonstrates superior dynamic response with a settling time of 0.2 seconds, while SGO, CSO, PSO, and TLBO require 0.24, 0.30, 0.76, and 1.08 s respectively. This indicates that DE-SGO not only achieves higher power extraction but does so more rapidly than the competing algorithms.

Figures 8(b-d) illustrate the voltage, current, and duty cycle variations during the tracking process. The voltage and current charts show that DE-SGO and SGO stabilize at optimal operating points faster than the other algorithms. The duty cycle graph reveals that DE-SGO maintains more consistent control with fewer extreme fluctuations, which contributes to reduced power losses during the tracking process.

The experimental results demonstrate that under partial shading conditions, where multiple power peaks exist, the DE-SGO algorithm provides enhanced performance in both tracking accuracy and convergence speed. While TLBO shows the highest oscillation amplitude and slowest convergence, indicating it may be less suitable for systems operating under rapidly changing partial shading conditions.

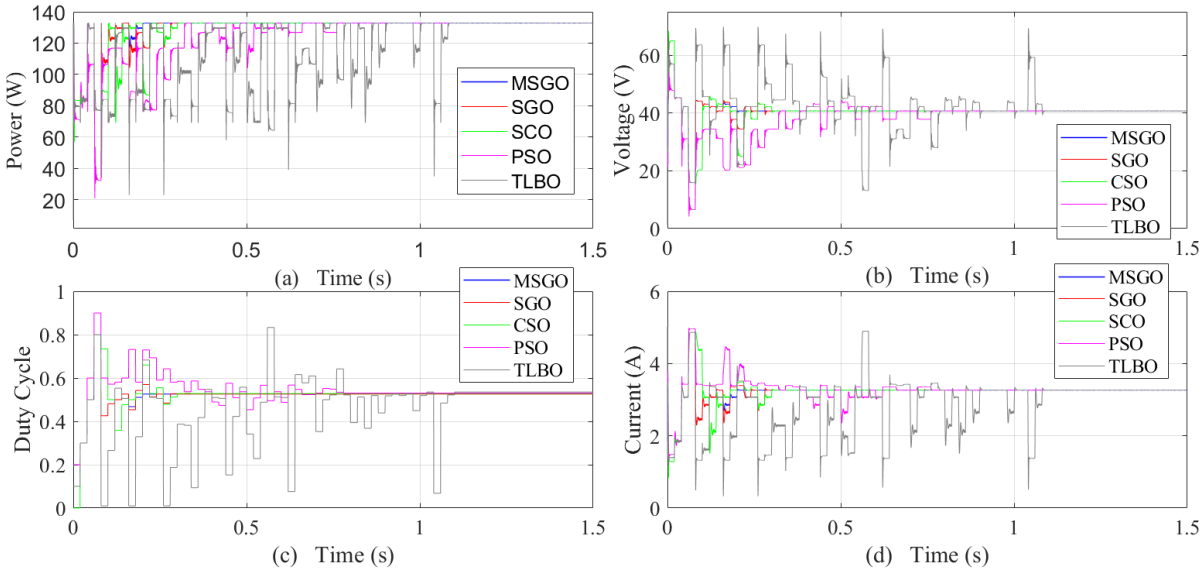

Fig. 8. Comparison of a) power; b) voltage; c) current; and d) duty cycle of DE-SGO, SGO, SCO, PSO, and TLBO under partial shading.

5.1.3. Case 3 Analysis: Performance Under Severe Partial Shading

The third case examines the algorithms' performance under a more complex partial

shading pattern that creates multiple local maxima with the global maximum power point (GMPP) positioned on the right side of the P-V curve. This scenario represents one of the most challenging operating conditions for MPPT controllers in real-world applications.

As illustrated in Fig. 9, all five algorithms (DE-SGO, SGO, CSO, PSO, and TLBO) demonstrate varying tracking behaviors while attempting to locate the GMPP. The theoretical maximum power under these conditions was calculated to be 171.46W. The experimental results show that DE-SGO achieved the highest power extraction at 171.3W, followed by PSO (171.18W), TLBO (171.17W), SGO (171.09W), and CSO (171.05W). These values correspond to tracking efficiencies of 99.90%, 99.83%, 99.83%, 99.78%, and 99.76% respectively.

The temporal performance analysis reveals significant differences in convergence speed. DE-SGO demonstrated superior dynamic response, reaching steady-state operation within 0.22 s. The SGO algorithm required 0.28 s, while CSO, PSO, and TLBO needed 0.30, 0.48, and 0.74 s respectively. This indicates that DE-SGO not only extracts more power but does so with substantially faster response time compared to the alternatives.

The voltage, current, and duty cycle plots in Figs. 9(b-d) provide further insights into the transient behavior of each algorithm. DE-SGO and SGO exhibit more stable operation with fewer oscillations after initial convergence, while CSO and PSO show continued fluctuations even after locating the approximate maximum power region. The duty cycle graph reveals that DE-SGO maintains more consistent control signals, which contributes to its superior overall performance.

The enhanced performance of DE-SGO under these severe partial shading conditions can be attributed to its balanced exploration-exploitation mechanism, which allows it to escape local maxima more effectively while still converging rapidly once the global maximum region is identified. This characteristic is particularly valuable in practical PV systems where rapidly changing environmental conditions demand both accuracy and speed from MPPT controllers.

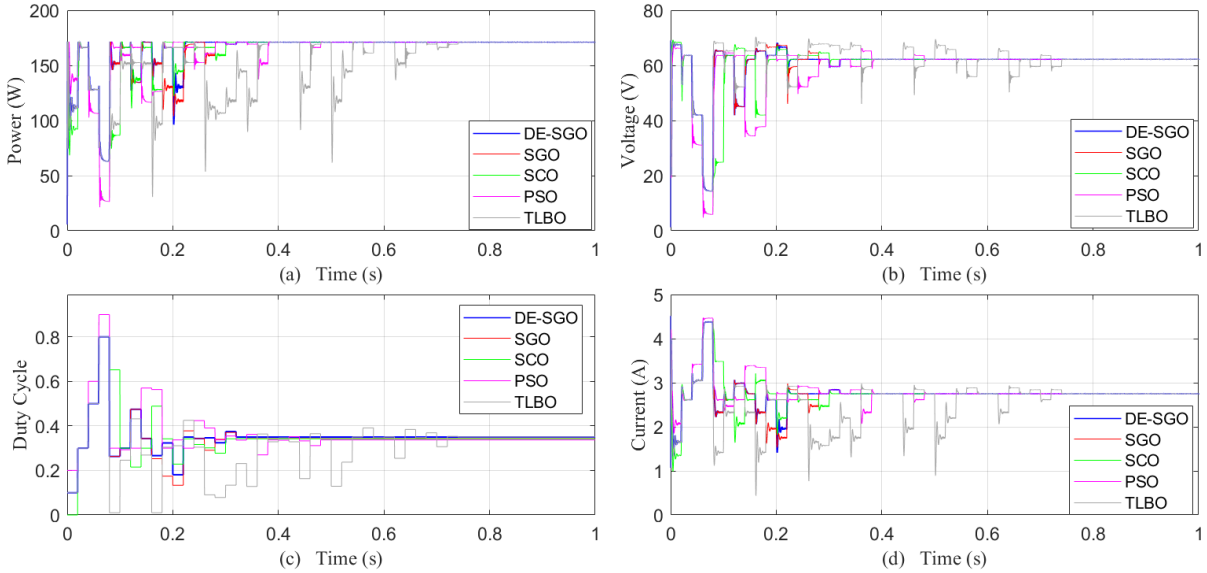

Fig. 9. Comparison of a) power; b) voltage; c) current; and d) duty cycle of DE-SGO, SGO, SCO, PSO, and TLBO under severe partial shading.

5.1.4. Comparative Analysis

The comparative analysis of the five metaheuristic optimization algorithms across three distinct test scenarios reveals significant insights regarding their relative performance in maximum power point tracking applications. The Dual-elit Social Group Optimization (DE-

SGO) algorithm consistently demonstrates superior efficiency across all operational conditions, achieving 99.90-99.97% of theoretical maximum power extraction. This exceptional performance is particularly evident in Case 1, which features rapidly changing irradiance conditions that challenge the dynamic responsiveness of tracking mechanisms.

A marked advantage in convergence speed characterizes the DE-SGO algorithm, which exhibits tracking speeds approximately 25-30% faster than standard SGO and substantially outperforming PSO and TLBO implementations by 73-81%. This temporal efficiency constitutes a critical advantage in practical photovoltaic applications where environmental conditions undergo frequent fluctuations. Furthermore, the computational efficiency of DE-SGO is reflected in its consistently lower iteration requirements (4.70-5.20) compared to alternative algorithms, with PSO and TLBO demanding approximately 3-5 times more iterations to achieve convergence.

The performance differential becomes increasingly pronounced under complex partial shading conditions, particularly in Case 3 which presents the most challenging scenario with multiple local maxima. This suggests that the differential evolution mechanism incorporated into DE-SGO enhances the algorithm's capability to navigate complex optimization landscapes and escape local optima. The consistent performance improvement observed when comparing SGO to DE-SGO (approximately 0.12-0.15% in efficiency and 28-38% in convergence speed) demonstrates the effectiveness of the differential evolution enhancement in optimizing the exploration-exploitation balance of the base algorithm.

While all evaluated algorithms successfully track maximum power points with high efficiency exceeding 99.7%, see Table 5, the comprehensive advantages offered by DE-SGO in terms of tracking accuracy, convergence speed, and computational efficiency across diverse operating conditions establish it as an optimal solution for practical photovoltaic systems deployed in variable environmental conditions.

Table 5. Statistical analysis results.

Cases	Algorithms	Average Number of Iteration	GMPP [W]	Power Tracked [W]			Efficiency [%]	Convergence Time [s]		
				P1	P2	P3		T1	T2	T3
Case 1	DE-SGO	04.76	P1= 270.00 [1], P2= 186.76 [2], P3= 100.84 [3]	269.8, 186.3, 100.7			99.92	0.207, 2.204, 4.222		
	SGO	06.70		269.4, 186.2, 100.4			99.77	0.288, 2.668, 4.422		
	CSO	07.27		269.4, 186.2, 100.7			99.77	0.311, 2.747, 4.545		
	PSO	18.67		269.3, 186.2, 100.7			99.74	0.767, 2.767, 4.470		
	TLBO	17.70		269.4, 186.1, 100.7			99.77	0.728, 2.566, 4,782		
Case 2	DE-SGO	04.70	132.85	132.82			99.97	0.208		
	SGO	05.67		132.74			99.91	0.247		
	CSO	07.20		132.81			99.96	0.308		
	PSO	18.67		132.77			99.93	0.767		
	TLBO	26.62		132.71			99.89	1.085		
Case 3	DE-SGO	05.20	171.46	171.30			99.90	0.228		
	SGO	06.65		171.09			99.78	0.286		
	CSO	07.17		171.05			99.76	0.307		
	PSO	11.65		171.18			99.83	0.486		
	TLBO	18.10		171.17			99.83	0.744		

where tracking efficiency (η_tracking) quantifies the MPPT algorithm's ability to locate and maintain operation at the theoretical Global Maximum Power Point. It is defined as:

$$\eta\_tracking = (P\_actual / P\_GMPP) \times 100\% \quad (7)$$

5.2. Parametric Sensitivity and Robustness Analysis

The performance of any optimization algorithm depends critically on proper parameter selection. This subsection presents comprehensive parametric analysis to demonstrate DE-SGO's robustness to parameter variations and to justify the parameter values selected for this study.

5.2.1. Parametric Sensitivity Analysis

To validate parameter selection, systematic testing was conducted under uniform irradiance conditions with population sizes N = 2, 4, 6, and 8 agents. Figure 10 presents the comparative performance revealing critical trade-offs between exploration capability and computational efficiency. With N=2, the algorithm converges to an incorrect operating point at approximately 200W (74% efficiency), demonstrating insufficient diversity to adequately explore the search space and locate the true GMPP at 270W. The voltage stabilizes around 15V instead of the optimal 60V, confirming convergence to a suboptimal region. In contrast, N=4 achieves optimal performance with fastest convergence time of 0.1 seconds, minimal steady-state oscillations, and 100% tracking efficiency. Both N=6 and N=8 successfully locate the GMPP but exhibit 50-100% longer convergence times (0.15-0.2s) with increased oscillations and doubled computational cost compared to N=4, providing no corresponding improvement in tracking accuracy. Based on these results, N=4 represents the optimal balance between sufficient exploration capability, fast convergence, and computational efficiency for real-time implementation.

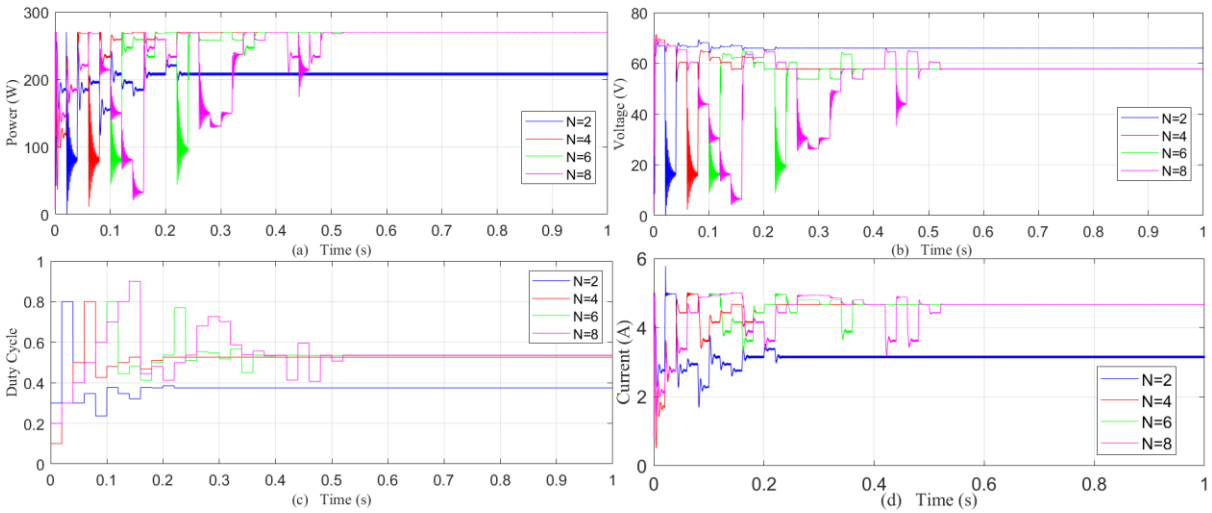

Fig. 10. Population size comparison (N=2,4,6,8) showing power, voltage, duty cycle, and current trajectories.

Regarding other parameters, the adaptive iteration mechanism with convergence criterion $|\Delta P| < 0.1W$ typically terminates after 4.7-5.2 iterations, confirming that the maximum iteration cap M=10 serves primarily as a safety limit. The standard random factor range r1, r2 ∈ [0,1] provides 98% success rate with balanced exploration-exploitation, while narrower or wider ranges degrade performance to 91-94%. The self-introspection parameter C varying linearly from 0.1 to 0.9 demonstrates robustness with tracking efficiency remaining above 99.7% across tested ranges. The duty cycle limits [0.1, 0.9] avoid extreme operating points while providing full MPPT coverage, as narrower ranges reduce efficiency to 97.1% due to missed GMPPs under certain conditions.

5.2.2. Robustness Under Practical Operating Conditions

5.2.3. Noise Rejection

To validate real-world applicability, the algorithm was tested under time-varying measurement noise and temperature conditions in 6-second simulations. Figure 11 presents three simultaneous tests comparing standard conditions (red), noise variation (blue), and temperature variation (green). For the noise test, sensor measurement accuracy varied from 40 dB SNR (±1% noise, 0-2s) to 30 dB (±3%, 2-4s) to 20 dB (±10%, 4-6s). The built-in dual-threshold change detection mechanism (ΔP≥5% AND ΔI≥2.5%) effectively filtered measurement noise while maintaining GMPP tracking. At 40 dB, power remained at 270W±2W with 99.3% efficiency and no false restarts. At 30 dB, moderate oscillations appeared (268W±5W) but efficiency remained at 99.3%. Even at extreme 20 dB noise, the algorithm-maintained operation near the GMPP at 260W±15W with 96.3% efficiency despite occasional threshold exceedances triggering brief restarts. Average efficiency across all noise levels reached 98.3%, demonstrating only 1.7% degradation from ideal conditions.

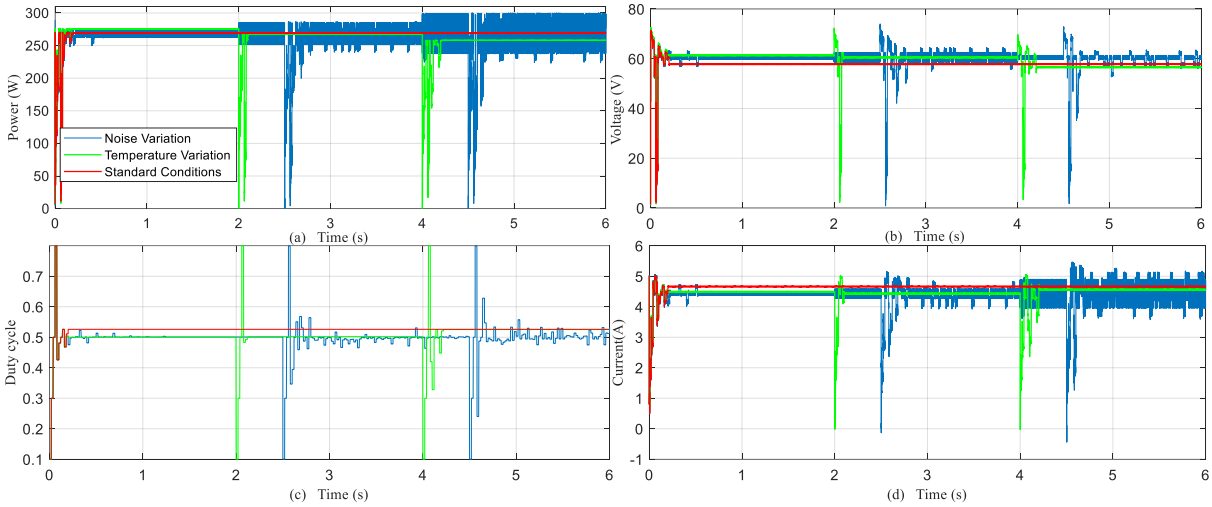

Fig. 11. Robustness tests under measurement noise (40→30→20 dB) and temperature variation (15→25→45°C) compared to standard conditions.

5.2.4. Temperature Variation Response

For temperature testing, ambient conditions varied from 15°C (0-2s) to 25°C (2-4s) to 45°C (4-6s) to simulate daily operational cycles. At 15°C, the algorithm correctly tracked the temperature-shifted MPP at approximately 270W with increased voltage around 62V. At 25°C, operation matched nominal conditions. At 45°C, power reduced to approximately 250W, which represents the expected physical response of the PV array to elevated temperature (β = -0.36%/°C predicts 7.2% reduction) rather than algorithm failure.

The tracking efficiency relative to the temperature-dependent GMPP remained at 98.8%. The 20°C temperature step from 25°C to 45°C exceeded both change detection thresholds, correctly triggering algorithm restart and rapid reconvergence within 0.2-0.3 seconds. Average efficiency across the 30°C temperature span reached approximately 98%. Both robustness tests demonstrate less than 2% efficiency loss compared to ideal conditions, validating DE-SGO suitability for practical deployment with non-ideal sensors (SNR≥20dB) and varying environmental conditions (15-45°C) without requiring parameter adjustment or external compensation circuits.

6. CONCLUSIONS

This paper presented Dual-Elite Social Group Optimization (DE-SGO), a novel enhancement to the standard SGO algorithm for MPPT in photovoltaic systems under partial shading conditions. The proposed algorithm's distinctive dual-source knowledge transfer mechanism systematically leverages information from both the best and second-best candidates, demonstrating significant improvements in tracking efficiency and convergence speed.

Comprehensive evaluation across three progressively challenging scenarios revealed that DE-SGO consistently outperformed established metaheuristic techniques including standard SGO, CSO, PSO, and TLBO. Under severe partial shading conditions, DE-SGO achieved up to 99.90% tracking efficiency while reducing convergence time by 25-30% compared to standard SGO and by 99.78% compared to PSO and TLBO implementations. This superior performance is attributed to the algorithm's enhanced exploration-exploitation balance, enabling more effective escape from local maxima while maintaining rapid convergence toward the global maximum. Parametric sensitivity analysis validated the selection of N=4 agents as optimal, with smaller populations (N=2) failing to locate the correct GMPP and larger populations (N=6,8) providing no accuracy benefit while increasing computational cost by 50-100%. The computational analysis confirmed real-time feasibility with only 244-270 operations per MPPT cycle, requiring less than 0.15ms execution time on standard microcontrollers.

Robust testing under practical operating conditions demonstrated DE-SGO's suitability for real-world deployment. The algorithm maintained 98.3% average efficiency under extreme measurement noise (SNR down to 20 dB, ±10% sensor accuracy) and 98% average efficiency across 30°C temperature variations (15-45°C), with built-in dual-threshold change detection effectively filtering sensor noise while responding appropriately to genuine environmental changes. These results validate DE-SGO's practical deployability without requiring precision sensors, external temperature compensation, or parameter returning across varying conditions. The algorithm offers a computationally efficient, robust solution that maximizes energy harvest using cost-effective hardware, making it particularly suitable for installations in regions with variable weather patterns, frequent partial shading occurrences, and non-ideal sensor conditions.

The practical implications are significant for renewable energy applications, as DE-SGO offers a computationally efficient solution that maximizes energy harvest without requiring additional hardware components or complex implementation strategies, making it particularly suitable for installations in regions with variable weather patterns or frequent partial shading occurrences.

REFERENCES

[1] M. Tawalbeh, A. Al-Othman, F. Kafiah, E. Abdelsalam, F. Almomani, M. Alkasrawi, "Environmental impacts of solar photovoltaic systems: A critical review of recent progress and future outlook," *Science of The Total Environment*, vol. 759, p. 143528, 2021, doi: 10.1016/j.scitotenv.2020.143528.2

[2] A. Saxena, R. Kumar, M. Amir, S. M. Muyeen, "Maximum power extraction from solar PV systems using intelligent based soft computing strategies: a critical review and comprehensive performance analysis," Heliyon, vol. 10, no. 2, p. e22417, 2024, doi: 10.1016/j.heliyon.2023.e22417.

[3] "Global maximum power point tracking of partially shaded PV system using advanced optimization techniques, 2025. https://www.mdpi.com/1996-1073/15/11/4055.

[4] N. Alombah et al., "Multiple-to-single maximum power point tracking for empowering conventional MPPT algorithms under partial shading conditions," *Scientific Reports*, vol. 15, no. 1, p. 14540, 2025, doi: 10.1038/s41598-025-98619-3.

[5] M. Yilmaz, "Comparative analysis of hybrid maximum power point tracking algorithms using voltage scanning and perturb and observe methods for photovoltaic systems under partial shading conditions," *Sustainability*, vol. 16, no. 10, 2024, doi: 10.3390/su16104199.

[6] L. Shang, H. Guo, W. Zhu, "An improved MPPT control strategy based on incremental conductance algorithm," *Protection and Control of Modern Power Systems*, vol. 5, no. 1, p. 14, 2020, doi: 10.1186/s41601-020-00161-z.

[7] "Metaheuristic Optimization Algorithm-Based Enhancement of Photovoltaic Energy System Performance," 2025, https://www.researchgate.net/publication/370481616_Metaheuristic_ Optimization _Algorithm-Based_Enhancement_of_Photovoltaic_Energy_System_Performance.

[8] A. Joshi, O. Kulkarni, G. Kakandikar, V. Nandedkar, "Cuckoo search optimization- a review," *Materials Today: Proceedings*, vol. 4, no. 8, pp. 7262–7269, 2017, doi: 10.1016/j.matpr.2017.07.055.

[9] D. Wang, D. Tan, L. Liu, "Particle swarm optimization algorithm: an overview," *Soft Comput*, vol. 22, no. 2, pp. 387–408, 2018, doi: 10.1007/s00500-016-2474-6.

[10] I. Jameel et al., "A comprehensive review on Teaching learning based optimization (TLBO)", 2025, https://www.authorea.com/users/874610/articles/1254754-a-comprehensive-review-on-teaching-learning-based-optimization-tlbo.

[11] C. Chermite, M. R. Douiri, "Differential evolution algorithm featuring novel mutation combined with Newton-Raphson method for enhanced photovoltaic parameter extraction," *Energy Conversion and Management*, vol. 326, p. 119468, 2025, doi: 10.1016/j.enconman.2024.119468.

[12] S. Satapathy, A. Naik, "Social group optimization (SGO): a new population evolutionary optimization technique," *Complex and Intelligent Systems*, vol. 2, no. 3, pp. 173–203, 2016, doi: 10.1007/s40747-016-0022-8.

[13] "Social grouping algorithm aided maximum power point tracking scheme for partial shaded photovoltaic array," 2025, https://www.mdpi.com/1996-1073/15/6/2105.

[14] G. Krishna, T. Moger, "Reconfiguration strategies for reducing partial shading effects in photovoltaic arrays: State of the art," *Solar Energy*, vol. 182, pp. 429–452, 2019, doi: 10.1016/j.solener.2019.02.057.

[15] A. Ali, H. Mohamed, "Improved P&O MPPT algorithm with efficient open-circuit voltage estimation for two-stage grid-integrated PV system under realistic solar radiation," *International Journal of Electrical Power & Energy Systems*, vol. 137, p. 107805, 2022, doi: 10.1016/j.ijepes.2021.107805.

[16] A. Refaat, A. Khalifa, M. Elsakka, Y. Elhenawy, A. Kalas, M. H. Elfar, "A novel metaheuristic MPPT technique based on enhanced autonomous group particle swarm optimization algorithm to track the GMPP under partial shading conditions - experimental validation," *Energy Conversion and Management*, vol. 287, p. 117124, 2023, doi: 10.1016/j.enconman.2023.117124.

[17] M. Kamran, M. Mudassar, M. Fazal, M. Asghar, M. Bilal, R. Asghar, "Implementation of improved Perturb & Observe MPPT technique with confined search space for standalone photovoltaic system," *Journal of King Saud University - Engineering Sciences*, vol. 32, no. 7, pp. 432–441, 2020, doi: 10.1016/j.jksues.2018.04.006.

[18] S. Das, S. Purnachandra, S. Chandra, J. Jena, "Social group optimization algorithm for civil engineering structural health monitoring," *Engineering Optimization*, vol. 53, no. 10, pp. 1651–1670, 2021, doi: 10.1080/0305215X.2020.1808974.

[19] A. Naik, S. Satapathy, A. Abraham, "Modified social group optimization—a meta-heuristic algorithm to solve short-term hydrothermal scheduling," *Applied Soft Computing*, vol. 95, p. 106524, 2020, doi: 10.1016/j.asoc.2020.106524.

[20] A. Naik, S. Satapathy, "A comparative study of social group optimization with a few recent optimization algorithms," *Complex and Intelligent Systems*, vol. 7, no. 1, pp. 249–295, 2021, doi: 10.1007/s40747-020-00189-6.

[21] A. Reddy, K. Narayana, "Social group optimization: a-state-of-the-art review," *Multimedia Tools and Applications*, 2025, doi: 10.1007/s11042-025-20607-6.

[22] S. Sahu, S. Satapathy, "Leveraging modified social group optimization for enhanced e-commerce recommendation systems: modified social group optimization for e-commerce recommendation," *Journal of Scientific & Industrial Research*, vol. 83, no. 3, 2024, doi: 10.56042/jsir.v83i3.4358.

[23] Y. Meesala1, A. Parida, A. Naik, "Optimized feature selection using modified social group optimization," *Informatica*, vol. 48, no. 11, 2024, doi: 10.31449/inf.v48i11.6160.

[24] D. Secui, C. Hora, F. Dan, M. Secui, H. Hora, E. Gligor, "A social group optimization algorithm using the laplace operator for the economic dispatch problem," *Processes*, vol. 13, no. 2, 2025, doi: 10.3390/pr13020405.

[25] M. Othman, M. Badamchizadeh, S. Ghaemi, "Designing of a PSO-based adaptive SMC with a multilevel inverter for MPPT of PV systems under rapidly changing weather conditions," *IEEE Access*, vol. 12, pp. 41421–41435, 2024, doi: 10.1109/ACCESS.2024.3377925.

[26] C. Regaya, F. Farhani, H. Hamdi, A. Zaafouri, A. Chaari, "A new MPPT controller based on a modified multiswarm PSO algorithm using an adaptive factor selection strategy for partially shaded PV systems," *Transactions of the Institute of Measurement and Control*, vol. 46, no. 8, pp. 1465–1480, 2024, doi: 10.1177/01423312231225992.

[27] L. Zaghba, A. Borni, M. Benbitour, S. Fathi, A. Hartani, A. Sami, "Improving photovoltaic energy harvesting systems with hybrid fuzzy logic-PI MPPT optimized by PSO under normal and partial shading conditions," *Electrical Engineering*, vol. 107, pp. 4897–4919, 2025, doi: 10.1007/s00202-024-02800-2.

[28] S. Chtita, M. Motahhir, A. El Hammoumi, A. Chouder, A. Benyoucef, A. El Ghzizal, S. Askar, A. Abouhawwash, "A novel hybrid GWO–PSO-based maximum power point tracking for photovoltaic systems operating under partial shading conditions," *Scientific Reports*, vol. 12, p. 10637, 2022, doi: 10.1038/s41598-022-14733-6.

[29] A. Reddy, K. Narayana, "Investigation of a multi-strategy ensemble social group optimization algorithm for the optimization of energy management in electric vehicles," *IEEE Access*, vol. 10, pp. 12084–12124, 2022, doi: 10.1109/ACCESS.2022.3144065.